

Fringe visibility and correlation in Mach—Zehnder interferometer with an asymmetric beam splitter

Yan-Jun Liu(刘彦军), Mei-Ya Wang(王美亚), Zhong-Cheng Xiang(相忠诚), and Hai-Bin Wu(吴海滨)
Citation: Chin. Phys. B, 2022, 31 (**11**): 110305. DOI: 10.1088/1674-1056/ac8c3b

What follows is a list of articles you may be interested in

Improvement of a continuous-variable measurement-device-independent quantum key distribution system via quantum scissors

Lingzhi Kong(孔令志), Weiqi Liu(刘维琪), Fan Jing(荆凡), Zhe-Kun Zhang(张哲坤), Jin Qi(齐锦), and Chen He(贺晨)
Chin. Phys. B, 2022, 31 (**9**): 090304. DOI: 10.1088/1674-1056/ac6dba

Photon blockade in a cavity-atom optomechanical system

Zhong Ding(丁忠) and Yong Zhang(张勇)
Chin. Phys. B, 2022, 31 (**7**): 070304. DOI: 10.1088/1674-1056/ac4cbc

Robustness of two-qubit and three-qubit states in correlated quantum channels

Zhan-Yun Wang(王展云), Feng-Lin Wu(吴风霖), Zhen-Yu Peng(彭振宇), and Si-Yuan Liu(刘思远)
Chin. Phys. B, 2022, 31 (**7**): 070302. DOI: 10.1088/1674-1056/ac4a61

Coherence migration in high-dimensional bipartite systems

Zhi-Yong Ding(丁智勇), Pan-Feng Zhou(周攀峰), Xiao-Gang Fan(范小刚),Cheng-Cheng Liu(刘程程), Juan He(何娟), and Liu Ye(叶柳)
Chin. Phys. B, 2022, 31 (**6**): 060308. DOI: 10.1088/1674-1056/ac48f8

Fringe visibility and distinguishability in two-path interferometer with an asymmetric beam splitter

Yanjun Liu(刘彦军), Jing Lu(卢竞), Zhihui Peng(彭智慧), Lan Zhou(周兰), Dongning Zheng(郑东宁)
Chin. Phys. B, 2019, 28 (**3**): 030303. DOI: 10.1088/1674-1056/28/3/030303

Fringe visibility and correlation in Mach–Zehnder interferometer with an asymmetric beam splitter

Yan-Jun Liu(刘彦军)[1], Mei-Ya Wang(王美亚)[1], Zhong-Cheng Xiang(相忠诚)[2], and Hai-Bin Wu(吴海滨)[1,†]

[1] *College of Physics, Mechanical and Electronical College, Shijiazhuang University, Shijiazhuang* 050035, *China*
[2] *Institute of Physics, Chinese Academy of Sciences, Beijing* 100190, *China*

(Received 29 May 2022; revised manuscript received 31 July 2022; accepted manuscript online 24 August 2022)

We study the wave–particle duality in a general Mach–Zehnder interferometer with an asymmetric beam splitter from the viewpoint of quantum information theory. The correlations (including the classical correlation and the quantum correlation) between the particle and the which-path detector are derived when they are in pure state or mixed state at the output of Mach–Zehnder interferometer. It is found that the fringe visibility and the correlations are effected by the asymmetric beam splitter and the input state of the particle. The complementary relations between the fringe visibility and the correlations are also presented.

Keywords: wave–particle duality, fringe visibility, correlation, general Mach–Zehnder interferometer

PACS: 03.67.–a, 03.65.Ta, 07.60.Ly **DOI:** 10.1088/1674-1056/ac8c3b

1. Introduction

A single quantum system has mutually exclusive properties, and these characteristics can be converted to each other depending on the method of observation, which is known as Bohr's complementarity principle.[1] The well-known example of the complementarity principle is wave–particle duality. A two-path interferometer, such as Young's double-slit or Mach–Zehnder interferometer (MZI), is used to quantify the wave–particle duality. The wave–like property and the particle-like property are shown by the fringe visibility and the which-path information (WPI) of the interferometer, respectively.[2–5] If the path of the particle is known accurately, the fringe visibility will disappear. The more WPI is obtained, the less the fringe visibility is. Recently, there have also been new advances of complementarity in experiments. QI *et al.*[6] experimentally constructed a weak-measurement MZI setup and performed a single-photon experiment with this new interferometer to test the wave–particle duality of photons. Yoon *et al.*[7] have proved that the experimental scheme using two stimulated parametric down-conversion processes is an ideal tool for investigating and understanding wave–particle duality and Bohr's complementarity quantitatively. Wang *et al.*[8] experimentally verified the duality relation between coherence and path information to the quantum case and revealed the effect of quantum superposition on the duality relation. Pozzobom *et al.*[9] performed experimental tests of these complementarity relations applied to a particular class of one-qubit quantum states and also for random quantum states of one, two, and three qubits. Dieguez *et al.*[10] predicted the existence of hybrid elements of reality interpolating between wave and particle by a quantum controlled device. The complementarity between the fringe visibility and the which-path knowledge has been studied greatly in the symmetric MZI (both beam splitters are symmetrical) in theory and experiment.[11–19] In addition, the complementary relationship in a general MZI with an asymmetric beam splitter (BS) has also attracted great attention.[20–29]

Originally, the uncertainty principle was attributed to the absence of interference fringe. Ever since the proposal that the entanglement is responsible for the loss of interference,[30] a detector is introduced to the MZI, which is capable of making the path taken by the interfering particle and called the which-path detector (WPD). The WPI is obtained by reading the state of the WPD. Although quantum entanglement is the great interest to quantum mechanics and the great importance to quantum information processing, it cannot explain all non-classical correlation,[31–33] which is called quantum correlation (QC). QC is more general and more fundamental than entanglement. Thus, it is reasonable to believe that not quantum entanglement but QC is responsible for the loss of interference. Liu *et al.*[18] have found that the correlation can quantify the particle-like property and obtained the relationship of the fringe visibility and the correlation in a symmetric MZI, but no one has studied the relationship between the correlation and the fringe visibility in a general MZI with an asymmetric BS. In this paper, we study both the wave-like property and the particle-like property in a general MZI with an asymmetric BS from the viewpoint of quantum information theory. The fringe visibility and the classical correlation (CC) or the QC are used to quantify the wave-like behavior and the particle-like behavior, respectively. The CC and the QC are calculated with either pure state or mixed state at the output of MZI. Here, the quan-

†Corresponding author. E-mail: 1102037@sjzc.edu.cn

© 2022 Chinese Physical Society and IOP Publishing Ltd

tum discord (QD) is used to represent the QC.[33] It is found that the fringe visibility and the correlations are effected by the asymmetric BS and the input state of the particle. The trade-off between the fringe visibility and the CC (QD) is also presented.

The paper is organized as follows. In Section 2, we present the MZI with an asymmetric BS, and the state of the particle and the WPD. In Section 3, we investigate the CC or QD of pure state and mixed state after the particle leaves the asymmetry MZI. The complementary relationships of the fringe visibility and the correlations are also presented. In Section 4, we made our conclusion.

2. Setups and state evolution

A general MZI consists of two BSs and two phase shifters(PSs) as shown in Fig. 1. The incident particles are split into two paths by the symmetrical beam splitter BS1. Orthogonal normalized states $|a\rangle$ and $|b\rangle$ are used to denote two possible paths, which support a two-dimensional Hilbert space. When the particles propagate in these two paths, PS1 and PS2 perform an rotation

$$U_{\rm P}(\phi) = \exp(-{\rm i}\phi\sigma_z) \tag{1}$$

on the path qubit, where pauli matrix $\sigma_z = |b\rangle\langle b| - |a\rangle\langle a|$. Finally, these two paths are recombined by the asymmetric beam splitter BS2. The effect of the BS2 on the particle is denoted by

$$U_{\rm B}(\beta) = \exp\left(-{\rm i}\frac{\beta}{2}\sigma_y\right), \tag{2}$$

which is equivalent to performing a rotation around the y axis by angle β. The BS2 is symmetrical when $\beta = \pi/2$.

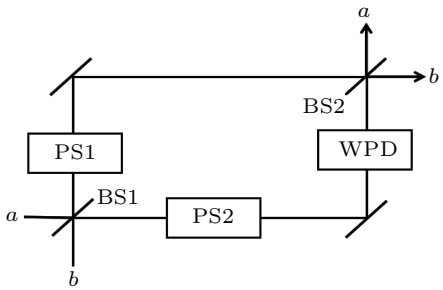


Fig. 1. The schematic sketch of the general Mach–Zehnder interferometer with the second BS asymmetry, a WPD is placed in path a.

To obtain the WPI, a WPD is placed on path a. When a particle initially in state

$$\rho_{\rm in}^{\rm Q} = \frac{1}{2}(1 + S_x\sigma_x + S_y\sigma_y + S_z\sigma_z) \tag{3}$$

goes through the MZI, the operator $M = |b\rangle\langle b|\otimes I + |a\rangle\langle a|\otimes U$ is performed on the initial state $\rho_{\rm in}^{\rm D}$ of WPD, where I and U are the identical and unitary operator, respectively. In Eq. (3), the Bloch vector $\boldsymbol{S} = (\boldsymbol{S}_x, \boldsymbol{S}_y, \boldsymbol{S}_z)$. After the particle has passed through the MZI, the state becomes

$$\begin{aligned}\rho_{\rm f}^{\rm QD} &= U_{\rm B}(\beta)MU_{\rm P}(\varphi)U_{\rm B}\left(\frac{\pi}{2}\right)\rho_{\rm in}^{\rm Q}\rho_{\rm in}^{\rm D}U_{\rm B}^{\dagger}(\frac{\pi}{2})U_{\rm P}^{\dagger}(\varphi)M^{\dagger}U_{\rm B}^{\dagger}(\beta)\\ &= \frac{1}{4}(1-S_x)(1+\sigma_z\cos\beta+\sigma_x\sin\beta)\otimes\rho_{\rm in}^{\rm D}\\ &\quad -\frac{1}{4}{\rm e}^{-{\rm i}\phi}(S_z-{\rm i}S_y)(\sigma_z\sin\beta-\sigma_x\cos\beta-{\rm i}\sigma_y)\otimes\rho_{\rm in}^{\rm D}U^{\dagger}\\ &\quad -\frac{1}{4}{\rm e}^{{\rm i}\phi}(S_z+{\rm i}S_y)(\sigma_z\sin\beta-\sigma_x\cos\beta+{\rm i}\sigma_y)\otimes U\rho_{\rm in}^{\rm D}\\ &\quad +\frac{1}{4}(1+S_x)(1-\sigma_z\cos\beta-\sigma_x\sin\beta)\otimes U\rho_{\rm in}^{\rm D}U^{\dagger}, \end{aligned}\tag{4}$$

and the reduced state of the WPD reads[27]

$$\rho_{\rm f}^{\rm D} = \omega_b\rho_{\rm in}^{\rm D} + \omega_a U\rho_{\rm in}^{\rm D}U^{\dagger}, \tag{5}$$

where

$$\omega_a = \frac{\cos^2(\beta/2)(1+S_x)}{1+S_x\cos\beta}, \quad \omega_b = \frac{\sin^2(\beta/2)(1-S_x)}{1+S_x\cos\beta}. \tag{6}$$

We note that the probabilities ω_a and ω_b are only dependent on the parameters S_x and β.

The probability that the particle is detected at output port a reads

$$\begin{aligned}p(\phi) &= {\rm tr}_{\rm QD}[\frac{1}{2}(1-\sigma_z)\rho_{\rm f}]\\ &= \frac{1}{2}(1+S_x\cos\beta)\\ &\quad +\frac{A}{2}\sqrt{S_z^2+S_y^2}\sin\beta\cos(\alpha+\gamma+\phi),\end{aligned}\tag{7}$$

where $A = |{\rm tr}_{\rm D}(U\rho_{\rm in}^{\rm D})|$, α and β are the phases of $S_x + {\rm i}S_y$ and ${\rm tr}_{\rm D}(U\rho_{\rm in}^{\rm D})$, respectively. The fringe visibility, which character the wave-like property of the particle, is defined via the probability in Eq. (7) as

$$\begin{aligned}V &\equiv \frac{\max P(\phi) - \min P(\phi)}{\max P(\phi) + \min P(\phi)}\\ &= \frac{A\sin\beta}{1+S_x\cos\beta}\sqrt{S_z^2+S_y^2},\end{aligned}\tag{8}$$

where the maximum and minimum are achieved by adjusting ϕ. We note that the expression of the fringe visibility measured in either output port a or b is different in an asymmetric MZI, however, the maximum of the fringe visibility remains the same no matter which port the particle is detected. The fringe visibility obtains the maximum A when the particle initially is in pure state and $\cos\beta = -S_x$.[27]

3. Information gain via general MZI

To obtain the WPI, a measurement on the WPD is necessary. For the convenience of calculation, we assume that the initial state of the WPD is in pure state denoted by $\rho_{\rm in}^{\rm D} = |r\rangle\langle r|$. For an arbitrary unitary operator U, states $|r\rangle$ and $|s\rangle \equiv U|r\rangle$ are linearly independent, which are either orthogonal state or non-orthogonal state. However, it is well known in quantum

measurement theory that non-orthogonal states cannot be accurately distinguished. If conclusive results are made, errors are unavoidable. Thence it is desirable to distinguish these states with minimum probability of error, which is denoted by the minimum error measurement.[34] Mathematically, the minimum error measurement for two-dimensional Hilbert space is characterized by the projective operators $\Pi_a^{\rm D} = |M_a\rangle\langle M_a|$ and $\Pi_b^{\rm D} = |M_b\rangle\langle M_b|$. For state in Eq. (5), the basis of the minimum error measurement reads

$$\begin{aligned} |M_a\rangle &= -\frac{1}{A_a\sqrt{1-A^2}}\left(\frac{1-\sqrt{1-4\omega_a\omega_b A^2}}{2\omega_a A}\right)|r\rangle \\ &\quad + \frac{1}{A_a\sqrt{1-A^2}}U|r\rangle, \\ |M_b\rangle &= -\frac{1}{A_b\sqrt{1-A^2}}\left(\frac{1+\sqrt{1-4\omega_a\omega_b A^2}}{2\omega_a A}\right)|r\rangle \\ &\quad + \frac{1}{A_b\sqrt{1-A^2}}U|r\rangle, \end{aligned} \tag{9}$$

where

$$\begin{aligned} A_a &= \sqrt{\frac{1-4\omega_a\omega_b A^2-\sqrt{1-4\omega_a\omega_b A^2}(1-2\omega_a A^2)}{2\omega_a^2 A^2(1-A^2)}}, \\ A_b &= \sqrt{\frac{1-4\omega_a\omega_b A^2+\sqrt{1-4\omega_a\omega_b A^2}(1-2\omega_a A^2)}{2\omega_a^2 A^2(1-A^2)}}. \end{aligned} \tag{10}$$

In fact, the bases in Eq. (9) are the eigenstates of the operator $\omega_a U\rho_{\rm in}^{\rm D}U^\dagger - \omega_b\rho_{\rm in}^{\rm D}$. In this section, after the particle leaves the asymmetry MZI, we will study the CC and QD between the particle and the WPD when they are in pure state or mixed state.

3.1. CC via general MZI

In quantum information theory, the CC[35] between the particle and the WPD can be expressed as

$$\mathcal{J}(\rho^{\rm QD}) = \max[S(\rho^{\rm Q}) - S(\rho^{\rm Q}|\{\Pi_k^{\rm D}\})], \tag{11}$$

where the $\rho^{\rm Q}$ is the reduced state of the particle, $S(\rho^{\rm Q})$ is the von Neumann entropy, $S(\rho^{\rm Q}|\{\Pi_k^{\rm D}\})$ is the quantum conditional entropy, $\Pi_k^{\rm D}$ is the measurement operator performed on the WPD.

(i) CC for the pure state at the output of MZI

We assume that the particle is entangled with the WPD after the particle leaves the MZI. They are in pure state

$$\rho_1^{\rm QD} = |\psi\rangle\langle\psi|, \tag{12}$$

where $|\psi\rangle = \sqrt{\omega_a}|a\rangle\otimes U|r\rangle + \sqrt{\omega_b}|b\rangle\otimes|r\rangle$. Since $\rho_1^{\rm QD}$ is in pure state, its quantum conditional entropy is equal to zero. It also means that when $\rho^{\rm QD}$ is pure state, the CC between the particle and the WPD does not depend on the measurement operator $\{\Pi_k^{\rm D}\}$. The CC between the particle and the WPD reads

$$\begin{aligned} \mathcal{J}(\rho_1^{\rm QD}) &= -\frac{B+\sqrt{B^2-\sin^2\beta(1-S_x^2)(1-A^2)}}{2B} \\ &\quad\times\log\frac{B+\sqrt{B^2-\sin^2\beta(1-S_x^2)(1-A^2)}}{2B} \\ &\quad -\frac{B-\sqrt{B^2-\sin^2\beta(1-S_x^2)(1-A^2)}}{2B} \\ &\quad\times\log\frac{B-\sqrt{B^2-\sin^2\beta(1-S_x^2)(1-A^2)}}{2B}, \end{aligned} \tag{13}$$

where $B = 1 + S_x\cos\beta$.

(ii) CC for the mixed state at the output of MZI

The state of the WPD and the particle is always in a superposition state due to the entanglement between them. A observer must subjectively select the state of the WPD and then read it out to obtain the WPI. In order to avoid the subjective selection, Zurek proposed "environment-induced superselection rules",[36] which is equivalent to introducing the environment into the original system. We can obtain the state of the particle and the WPD

$$\rho_2^{\rm QD} = \omega_a|a\rangle\langle a|\otimes U|r\rangle\langle r|U^\dagger + \omega_b|b\rangle\langle b|\otimes|r\rangle\langle r| \tag{14}$$

by tracing over the degree of the environment. The state $|a\rangle$ ($|b\rangle$) is correlated with the state $U|r\rangle$ ($|r\rangle$) due to the "environment-induced superselection". The observer can accurately know the state of the particle by reading out the state of the WPD. If the WPD is in the state $U|r\rangle$ ($|r\rangle$), the state of the particle is $|a\rangle$ ($|b\rangle$). Different from the $\mathcal{J}(\rho_1^{\rm QD})$, the $\mathcal{J}(\rho_2^{\rm QD})$ depends on the measurement basis. According to the numerical analysis, when the measurement basis $\Pi_k^{\rm D} = |M_k\rangle\langle M_k|$ induced by the environment is the same as the measurement basis vector used in error-minimum measurement, the quantum condition entropy $S(\rho^{\rm Q}|\{\Pi_k^{\rm D}\})$ obtains the minimum. The CC between the particle and the WPD reads

$$\begin{aligned} J(\rho_2^{\rm QD}) &= -\omega_b\log\omega_b - \omega_a\log\omega_a + \omega_a(S\sin\gamma - A\cos\gamma)^2 \\ &\quad\times\log\left[\frac{\omega_a(S\sin\gamma-A\cos\gamma)^2}{\omega_a(S\sin\gamma-A\cos\gamma)^2+\omega_b\cos^2\gamma}\right] \\ &\quad+\omega_b\cos^2\gamma\log\left[\frac{\omega_b\cos^2\gamma}{\omega_a(S\sin\gamma-A\cos\gamma)^2+\omega_b\cos^2\gamma}\right] \\ &\quad+\omega_a(A\sin\gamma+S\cos\gamma)^2 \\ &\quad\times\log\left[\frac{\omega_a(A\sin\gamma+S\cos\gamma)^2}{\omega_a(A\sin\gamma+S\cos\gamma)^2+\omega_b\sin^2\gamma}\right] \\ &\quad+\omega_b\sin^2\gamma\log\left[\frac{\omega_b\sin^2\gamma}{\omega_a(A\sin\gamma+S\cos\gamma)^2+\omega_b\sin^2\gamma}\right], \end{aligned} \tag{15}$$

where

$$\sin\gamma = -\frac{1}{A_b},\quad \cos\gamma = -\frac{1}{A_a}. \tag{16}$$

Equations (13) and (15) show that the $\mathcal{J}(\rho_1^{\rm QD})$ and the $\mathcal{J}(\rho_2^{\rm QD})$ are functions of the parameters S_x, β, and A, respectively. In Fig. 2, we plot $\mathcal{J}(\rho_1^{\rm QD})$ and $\mathcal{J}(\rho_2^{\rm QD})$ as a functions of S_x and β with parameter $A = 1/3$ in brown and blue, respectively. From Fig. 2, we can obtain the following conclusions. (i) The values of $\mathcal{J}(\rho_1^{\rm QD})$ and $\mathcal{J}(\rho_2^{\rm QD})$ first increase and then decrease as $S_x(\beta)$ increases for a given $\beta(S_x)$. (ii) The peak appears at $S_x = -1/2$ when $\beta = \pi/3$, $S_x = 0$ when $\beta = \pi/2$, $S_x = 1/2$ when $\beta = 2\pi/3$ in Fig. 2(b); $\beta = \pi/6$ when $S_x = -\sqrt{3}/2$, $\beta = \pi/2$ when $S_x = 0$, $\beta = 5\pi/6$ when $S_x = \sqrt{3}/2$ in Fig. 2(c). (iii) The value of the CC between the particle and the WPD is zero in the following situations. i) The effect of the BS2 for the particle is full transmission (full reflection), corresponding to $\beta = 0(\pi)$. ii) The particle only travels along the a (b) path, corresponding to $S_x = 1, (-1)$. In Fig. 3 (Fig. 4), we plot $\mathcal{J}(\rho_1^{\rm QD})$ and $\mathcal{J}(\rho_2^{\rm QD})$ as a function of $S_x(\beta)$ and A with parameter $\beta = \pi/6$ ($S_x = 1/2$) in brown and blue, respectively. The blue part shown in Figs. 2(a) and 4(a) indicates $\mathcal{J}(\rho_1^{\rm QD}) = \mathcal{J}(\rho_2^{\rm QD})$. From Figs. 3(b) and 4(b), one finds that $\mathcal{J}(\rho_1^{\rm QD})$ and $\mathcal{J}(\rho_2^{\rm QD})$ decrease as A increases. The peak appears at $S_x = -\sqrt{3}/2$ when $\beta = \pi/6$ in Fig. 3(c) and $\beta = 2\pi/3$ when $S_x = 1/2$ in Fig. 4(c). By analyzing Figs. 2–4, we can obtain the following two conclusions. The first is: under the same conditions, the relationship of $\mathcal{J}(\rho_1^{\rm QD})$ and $\mathcal{J}(\rho_2^{\rm QD})$ satisfies $\mathcal{J}(\rho_1^{\rm QD}) \geq \mathcal{J}(\rho_2^{\rm QD})$. The second is: the maximum of $\mathcal{J}(\rho_1^{\rm QD})$ and $\mathcal{J}(\rho_2^{\rm QD})$ can be achieved once as $\cos\beta = -S_x$. The $\mathcal{J}(\rho_1^{\rm QD})$ becomes the maximum

$$\mathcal{J}(\rho_1^{\rm QD})_{\rm max} = -\frac{1+A}{2}\log\left(\frac{1+A}{2}\right) - \frac{1-A}{2}\log\left(\frac{1-A}{2}\right), \tag{17}$$

when $\cos\beta = -S_x$.

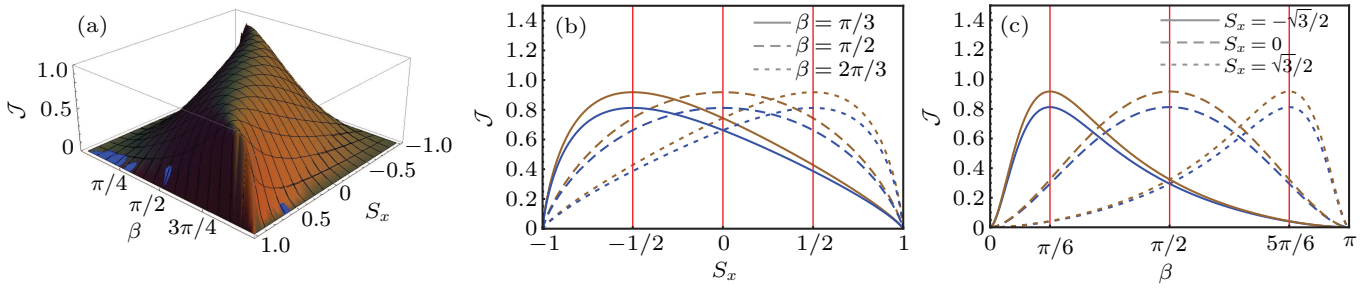


Fig. 2. (a) The CC $\mathcal{J}(\rho_1^{\rm QD})$ and $\mathcal{J}(\rho_2^{\rm QD})$ as functions of S_x and β with $A = 1/3$ are represented in brown and blue, respectively. (b) The cross section of the three-dimensional (3D) surface for $\beta = \pi/3, \pi/2, 2\pi/3$, (c) the cross section of the 3D surface for $S_x = -\sqrt{3}/2$, 0, $\sqrt{3}/2$.

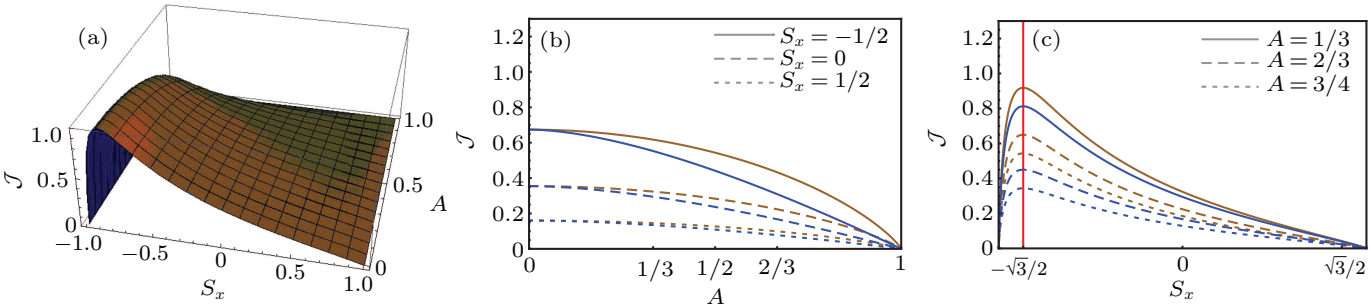


Fig. 3. (a) The CC $\mathcal{J}(\rho_1^{\rm QD})$ and $\mathcal{J}(\rho_2^{\rm QD})$ as functions of A and S_x with $\beta = \pi/6$ are represented in brown and blue, respectively. (b) The cross section of the 3D surface for $S_x = -1/2$, 0, 1/2, (c) the cross section of the 3D surface for $A = 1/3$, 2/3, 3/4.

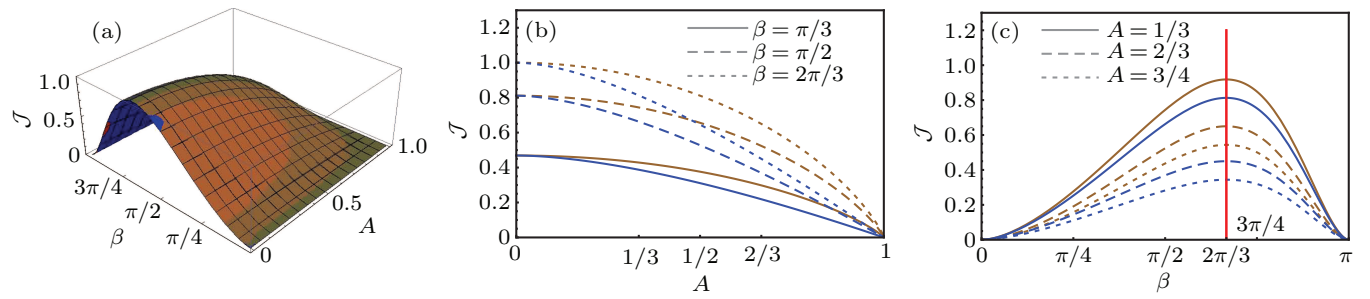


Fig. 4. (a) The CC $\mathcal{J}(\rho_1^{\rm QD})$ and $\mathcal{J}(\rho_2^{\rm QD})$ as functions of A and β with $S_x = 1/2$ are represented in brown and blue, respectively. (b) The cross section of the 3D surface for $\beta = \pi/3$, $\pi/2$, $2\pi/3$, (c) the cross section of the 3D surface for $A = 1/3$, 2/3, 3/4.

In Fig. 5, we plot $\mathcal{J}^2(\rho_1^{\rm QD})_{\rm max}+V_{\rm max}^2$ as a function of A. We find the relationship

$$\mathcal{J}^2(\rho_1^{\rm QD})_{\rm max}+V_{\rm max}^2\leq 1 \tag{18}$$

for any A. So, we can obtain the complementary relation of $\mathcal{J}(\rho_1^{\rm QD})$ and V

$$\mathcal{J}^2(\rho_1^{\rm QD})+V^2\leq 1. \tag{19}$$

Due to the relationship between $\mathcal{J}(\rho_1^{\rm QD})$ and $\mathcal{J}(\rho_2^{\rm QD})$, we can also obtain the complementarity relationship between $\mathcal{J}(\rho_2^{\rm QD})$ and V

$$\mathcal{J}^2(\rho_2^{\rm QD})+V^2\leq 1. \tag{20}$$

The equals sign holds in Eqs. (19) and (20) in the following situations. (I) The value of the fringe visibility is one, corresponding to $\cos\beta=-S_x$ and $V=1$. This means the state of WPD satisfies $|r\rangle=U|r\rangle$, the interference pattern is completely observed. (II) The value of $\mathcal{J}(\rho_1^{\rm QD})$ or $\mathcal{J}(\rho_2^{\rm QD})$ is one, corresponding to $\cos\beta=-S_x$ and $V=0$. This means the states $|r\rangle$ and $U|r\rangle$ are mutually orthogonal, a perfect WPI of the particle propagating is achieved.

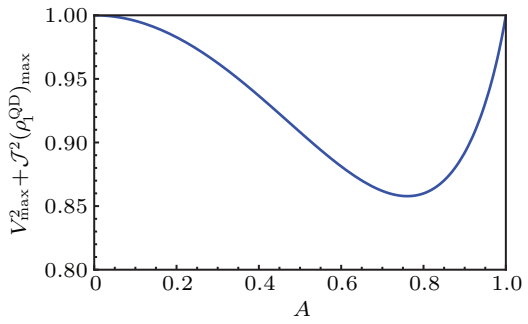


Fig. 5. The relationship between $\mathcal{J}^2(\rho_1^{\rm QD})_{\rm max}+V_{\rm max}^2$ and A.

3.2. QD via general MZI

The QD is usually used to denote QC, and QD between the particle and the WPD is defined as the total correlation minus CC

$$\mathcal{D}(\rho^{\rm QD})=I(\rho^{\rm QD})-\mathcal{J}(\rho^{\rm QD}), \tag{21}$$

here, quantum mutual information

$$I(\rho^{\rm QD})=S(\rho^{\rm Q})+S(\rho^{\rm D})-S(\rho^{\rm QD}) \tag{22}$$

is used to quantify the total correlation, where S is the von Neumann entropy, $\rho^{\rm Q}$ and $\rho^{\rm D}$ are reduced density matrixes of $\rho^{\rm QD}$.

(i) QD for pure state at output of MZI

By simple calculations, we can obtain QD as follows:

$$\mathcal{D}(\rho_1^{\rm QD})=\mathcal{J}(\rho_1^{\rm QD}) \tag{23}$$

between the particle and the WPD when their final state is in the pure state. From Eqs. (19) and (23), we obtain the complementary relation

$$\mathcal{D}^2(\rho_1^{\rm QD})+V^2\leq 1. \tag{24}$$

(ii) QD for mixed state at output of MZI

By Eq. (21), we can obtain that when the final state of particle and WPD is in a mixed state, the QD

$$\mathcal{D}(\rho_2^{\rm QD})=\mathcal{J}(\rho_1^{\rm QD})-\mathcal{J}(\rho_2^{\rm QD}). \tag{25}$$

From Eq. (25), we find that the total correlation of particle and WPD

$$I(\rho_2^{\rm QD})=\mathcal{J}(\rho_1^{\rm QD}). \tag{26}$$

Liu *et al.*[18] have demonstrated that $\mathcal{D}(\rho_2^{\rm QD})$ and V do not satisfy the complementarity relation when $S_x=-\cos\beta=0$ and the input particle is in the pure state. For the more general case we discuss in this section, when the final state of the particle and the WPD is in the mixed state, the $\mathcal{D}(\rho_2^{\rm QD})$ and V also do not satisfy the complementarity relation.

4. Conclusion

We have investigated the complementarity of the fringe visibility and CC or QD in an MZI with one asymmetric BS. The fringe visibility V exhibits an upper bound A when the particle initially is in the pure state and $\cos\beta=-S_x$. We solved the CC $\mathcal{J}(\rho_1^{\rm QD})$ and the QD $\mathcal{D}(\rho_1^{\rm QD})$ between the particle and the WPD when the final state of them is in the pure state, and found that $\mathcal{D}(\rho_1^{\rm QD})=\mathcal{J}(\rho_1^{\rm QD})$ and the maximum of $\mathcal{J}(\rho_1^{\rm QD})$ and $\mathcal{D}(\rho_1^{\rm QD})$ can be achieved when $\cos\beta=-S_x$. The CC $\mathcal{J}(\rho_1^{\rm QD})$ or the QD $\mathcal{D}(\rho_1^{\rm QD})$ and the fringe visibility V satisfy the complementarity relationship $\mathcal{J}^2(\rho_1^{\rm QD})(\mathcal{D}^2(\rho_1^{\rm QD}))+V^2\leq 1$. We also obtained the CC $\mathcal{J}(\rho_2^{\rm QD})$ and QD $\mathcal{D}(\rho_2^{\rm QD})$ between the particle and the WPD when the final state of them is in the mixed state. $\mathcal{J}(\rho_2^{\rm QD})$ can achieve the maximum once as $\cos\beta=-S_x$. The complementarity relationship between $\mathcal{J}(\rho_2^{\rm QD})$ and V satisfies $\mathcal{J}^2(\rho_2^{\rm QD})+V^2\leq 1$. It is also found that $\mathcal{J}(\rho_1^{\rm QD})$ $(\mathcal{D}(\rho_1^{\rm QD}))\geq\mathcal{J}(\rho_2^{\rm QD})$ $(\mathcal{D}(\rho_2^{\rm QD}))$, which means that the environment not only induces the optimal measurement basis, but also reduces the CC and QD between the particle and the WPD.

Acknowledgements

Project supported by the National Natural Science Foundation of China (Grant No. 11975095), the Natural Science Foundation of Hebei Province, China (Grant No. A2022106001) and Shijiazhuang University Doctoral Scientific Research Startup Fund Project (Grant No. 20BS023).

References

[1] Bohr N 1928 *Nature* **121** 580
[2] Wootters W K and Zurek W H 1979 *Phys. Rev. D* **19** 473
[3] Greenberger D M and Yasin A 1988 *Phys. Lett. A* **128** 391
[4] Jaeger G, Shimony A and Vaidman L 1995 *Phys. Rev. A* **51** 54
[5] Englert B G 1996 *Phys. Rev. Lett.* **77** 2154
[6] Qi F H, Wang Z Y, Xu W W, Chen X W and Li Z Y 2020 *Photon. Res.* **8** 622
[7] Yoon T H and Cho M 2021 *Sci. Adv.* **7** eabi9268
[8] Wang D Y, Wu J J, Ding J F, Liu Y W, Huang A Q and Yang X J 2021 *Entropy* **23** 122
[9] Pozzobom M B, Basso M L W and Maziero J 2021 *Phys. Rev. A* **103** 022212
[10] Dieguez P R, Guimares J R, Peterson J P S, Angelo R M and Serra R M 2021 arXiv: 2104.08152v2 [quant-ph]
[11] Mittelstaedt P, Prieu A and Schieder R 1987 *Found. Phys.* **17** 891
[12] Dürr S and Rempe G 2000 *Am. J. Phys.* **68** 1021
[13] Ban M 2008 *Mod. Opt.* **55** 3625
[14] Bana M, Shibataa F and Kitajimaa S 2009 *J. Mod. Opt.* **56** 89
[15] Liu N L, Li L, Yu S X and Chen Z B 2009 *Phys. Rev. A* **79** 052108
[16] Bosyk G M, Portesi M, Holik F and Plastino A 2013 *Phys. Scr.* **87** 065002
[17] Angelo R M and Ribeiro A D 2015 *Found. Phys.* **45** 1407
[18] Liu Y, Lu J and Zhou L 2017 *Opt. Express* **25** 202
[19] Verma H, Zych M and Costa F 2021 *Quantum* **5** 525
[20] Jacques V, Wu E, Grosshans F, Treussart F, Grangier P, Aspect A and Roch J F 2008 *Phys. Rev. Lett.* **100** 220402
[21] Han Y, Wang W C, Wei W, Chen P X and Li C Z 2009 *Chin. Phys. Lett.* **26** 040303
[22] Ionicioiu R and Terno D R 2011 *Phys. Rev. Lett.* **107** 230406
[23] Li L, Liu N L and Yu S X 2012 *Phys. Rev. A* **85** 054101
[24] Tang J S, Li Y L, Li C F and Guo G C 2013 *Phys. Rev. A* **88** 014103
[25] Guo Q, Cheng L Y, Wang H F and Zhang S 2015 *Int. J. Theor. Phys.* **54** 2517
[26] Long G L, Qin W, Yang Z and Li J L 2018 *Sci. China* **61** 030311
[27] Liu Y J, Lu J and Zhou L 2017 *Laser Phys. Lett.* **14** 055204
[28] Liu Y J, Lu J, Peng Z H, Zhou L and Zheng D N 2019 *Chin. Phys. B* **28** 030303
[29] Liu J Z, Liu Y J and Lu J 2019 *Chin. Phys. Lett.* **36** 050302
[30] Scully M O and Drühl K 1982 *Phys. Rev. A* **25** 2208
[31] Zurek W H 2000 *Ann. Phys.* (Leipzig) **9** 855
[32] Henderson L and Vedral V 2001 *J. Phys. A* **34** 6899
[33] Ollivier H and Zurek W H 2001 *Phys. Rev. Lett.* **88** 017901
[34] Chefles A 2000 *Contemp. Phys.* **41** 401
[35] Henderson L and V Vedral 2001 *J. Phys. A* **34** 6899
[36] Zurek W H 1982 *Phys. Rev. D* **26** 1862